

A fast and exact approach for stabilizer Rényi entropy via the XOR-FWHT algorithm

Xuyang Huang,^{1,*} Han-Ze Li,^{1,2,†} and Jian-Xin Zhong^{1,‡}

¹*Institute for Quantum Science and Technology, Shanghai University, Shanghai 200444, China*

²*Department of Physics, National University of Singapore, Singapore 117542, Singapore*

Quantum advantage is widely understood to rely on key quantum resources beyond entanglement, among which nonstabilizerness (quantum “magic”) plays a central role in enabling universal quantum computation. However, a direct brute-force enumeration of all Pauli strings and the corresponding expectation values from a length- 2^N state vector, where N is the system size, yields an overall computational cost scaling as $O(8^N)$, which quickly becomes infeasible as the system size grows. Here we reformulate the second-order stabilizer Rényi entropy in a bitstring language, expose an underlying XOR-convolution structure on \mathbb{Z}_2^N , and reduce the computation to 2^N fast Walsh-Hadamard transforms of length, together with pointwise operations, yielding a deterministic and exact XOR fast Walsh-Hadamard transforms algorithm with runtime scaling $O(N4^N)$ and natural parallelism. This algorithm enables high-precision, medium-scale exact calculations for generic state vectors. It provides a practical tool for probing the scaling, phase diagnostics, and dynamical fine structure of quantum magic in many-body systems.

I. INTRODUCTION

Quantum advantage refers to the possibility that a quantum computer achieves an exponential speedup over classical computation for specific tasks. This capability is commonly understood within the framework of resource theories [1] in which a set of key quantum resources collectively underpins computational advantage [1–6]. Among the resources most closely tied to quantum advantage are entanglement [7, 8] and *nonstabilizerness* [9–62], which is also known as quantum *magic*. These resources are widely regarded as necessary ingredients for universal quantum computation [63], and they play a central role in the construction and optimization of practical quantum devices [64–67]. It is important to emphasize that strong entanglement alone does *not* guarantee quantum advantage, since stabilizer states can be highly entangled while remaining efficiently simulable on classical computers under the Gottesman-Knill theorem [68, 69]. Nonstabilizerness, therefore, serves as an independent resource that quantifies the departure from the stabilizer manifold and that reflects the consumption of non-Clifford resources required to prepare a given state, which is why it is viewed as a particularly scarce and crucial resource for universal quantum computation when non-Clifford operations are costly in experiments and in fault-tolerant architectures [70–74].

In recent years, the behavior of magic and related nonstabilizerness quantifiers in many-body quantum systems has also become an active topic at the interface of quantum information [75–88] and many-body physics [80, 84, 89–135]. Quantifying nonstabilizerness is *challenging* both conceptually and computationally. A broad range of magic measures has been proposed, which includes quantifiers based on quasiprobability representations, robustness-type measures, and measures related to operational or simulation overhead [136–142]. For generic many-body states, however, evaluating these quanti-

fiers typically entails *exponential* computational cost, which severely limits their applicability to larger system sizes.

The stabilizer Rényi entropies (SREs) [11], provide a complementary perspective for quantifying nonstabilizer resources [11, 143]. Since SREs form a family of rigorously established magic monotones [144], they avoid the need to construct a nonstabilizer decomposition explicitly, and because they are expressed directly in terms of Pauli statistics, they provide an attractive bridge between theory, numerics, and measurement-based evaluation protocols. Among the different orders, the second-order SRE (2-SRE) is distinguished as the simplest nontrivial SRE and because it has an explicit polynomial structure expressible as a quartic sum of Pauli expectation values. For an N -qubit pure state $|\psi\rangle$ in a Hilbert space of dimension d , the 2-SRE is defined as

$$\mathcal{M}_2(|\psi\rangle) = -\log\left(\frac{1}{d} \sum_{P \in \mathcal{P}_N} |\langle\psi|P|\psi\rangle|^4\right), \quad (1)$$

where \mathcal{P}_N denotes the set of N -qubit Pauli strings, which is understood modulo an overall phase since such phases do not affect the modulus in (1). This expression can be interpreted as a *fourth-moment* concentration of Pauli expectation values, so that \mathcal{M}_2 becomes smaller when the Pauli statistics are highly structured, as in stabilizer states, and becomes larger when the distribution is more spread, as in generic nonstabilizer states.

Despite the explicit form of (1), its direct numerical evaluation remains *prohibitively* expensive. The summation runs over an exponentially large set of Pauli strings whose cardinality scales as $|\mathcal{P}_N| \sim 4^N$, and for a *generic state-vector* input, computing a single expectation value $\langle\psi|P|\psi\rangle$ typically requires a full summation over d amplitudes. As a consequence, the brute-force enumerated approach (Hereinafter referred to as brute-force approach) is often characterized by an overall scaling of $O(8^N)$, which in practice confines exact calculations for spin- $\frac{1}{2}$ systems to relatively small system sizes, usually $N \lesssim 14$. This limitation is structural rather than technical and constitutes a central computational bottleneck in many-body studies of nonstabilizerness, as it severely restricts controlled access to scaling behaviour, phase diagnostics, and dy-

* hxy@shu.edu.cn

† hanzeli@u.nus.edu

‡ jxzhong@shu.edu.cn

namical phenomena at larger N .

To overcome this bottleneck, several computational strategies have been developed for the 2-SRE and related quantities. (i). Tensor-network approaches can be practical when the state admits a low-entanglement representation or an effectively controlled bond dimension [48, 51, 57, 145–153], and their accuracy is then limited primarily by the fidelity of the underlying state representation when truncations are required. (ii). Sampling-based and Monte-Carlo estimators [96, 154–157] avoid the complete 4^N enumeration by trading deterministic accuracy for statistical uncertainty, and their efficiency is governed by variance control and autocorrelation properties. (iii). For states with special algebraic structure, such as Gaussian states [54, 89, 91, 158–161], one can exploit reduced descriptions in terms of covariance matrices to obtain substantially faster evaluations. However, the applicability is then restricted to those structured families. These methods are powerful within their respective regimes. Still, their applicability and accuracy degrade outside their domain, as they typically rely on low-entanglement structures, controlled-variance stochastic estimators, or special state manifolds. There is an urgent need for a 2-SRE numerical method that does not assume special structure, yet remains broadly applicable, deterministically accurate, and computationally efficient by exploiting the algebraic structure intrinsic to (1).

In this work, we address this gap by presenting a deterministic and exact algorithm for evaluating the 2-SRE of a generic N -qubit pure state given as a state vector. We systematically rewrite the Pauli-string summation in (1) in a bitstring form and expose a convolution and correlation structure over the group \mathbb{Z}_2^N , i.e., XOR-convolutions [162] and correlations over bitstrings, which allows us to leverage orthogonality identities and the convolution theorem associated with the Walsh-Hadamard transform (WHT). This yields an exact formula amenable to efficient numerical implementation, in which the computation reduces to repeated fast Walsh-Hadamard transforms (FWHTs), pointwise operations, and index reshuffling. Accordingly, we refer to the algorithm proposed in this work as the *XOR-FWHT* algorithm. The algorithm requires Hilbert space of dimension $d = 2^N$ FWHTs of length d , achieves a runtime scaling of $O(N4^N)$ with modest additional memory, and is naturally parallelizable over the shift index. This reduction yields a substantial improvement over brute-force Pauli enumeration and enables exact evaluation of the 2-SRE up to $N \sim 20$ for generic state vectors. While fast Walsh-Hadamard methods and \mathbb{Z}_2^N convolution structures have been widely used in algorithm design and related computations involving quantum operators [163], we provide a dedicated, systematic derivation of the 2-SRE and an open-source implementation of the resulting method.

The structure of this work is organized as follows. In Sec. II, starting from Eq. (1), we present a detailed derivation. After representing Pauli strings as bitstrings, we systematically simplify the expression by means of XOR convolution and the WHT, ultimately arriving at a compact form that is well suited for numerical implementation and exhibits significantly improved computational efficiency. In Sec. III, we provide the pseudocode of the proposed XOR-FWHT algo-

rithm, and present the corresponding Python implementation details in the Appendix, together with benchmarks of the actual runtime performance on multicore CPU architectures. In Sec. IV, we present a series of numerical applications, which verify the consistency of our algorithm with both theoretical predictions and brute-force approaches; moreover, the high numerical precision of the method enables it to resolve subtle effects arising from small parameter variations in physical models. Finally, in Sec. V, we summarize the main results of this work and discuss potential directions for future developments of the XOR-FWHT algorithm.

II. ALGEBRAIC REFORMULATION OF THE 2-SRE

In this section, we derive Eq. (1), which constitutes the foundation of the numerical algorithm.

Bitstring representation of Pauli strings. The set of single-qubit Pauli operators is $\{1, X, Y, Z\}$. Noting that $Y = iXZ$, and that the overall phase of a Pauli string does not affect $|\langle \psi | P | \psi \rangle|^4$, we may, without loss of generality, ignore the global phase of Pauli strings in what follows and retain only their $X^x Z^z$ structure.

Any N -qubit Pauli string can be uniquely written as

$$P = X_1^{x_1} \cdots X_N^{x_N} Z_1^{z_1} \cdots Z_N^{z_N} \equiv X^x Z^z, \quad (2)$$

where $x := (x_1, \dots, x_N)$, $z := (z_1, \dots, z_N) \in \mathbb{Z}_2^N$. Therefore, summing over all Pauli strings $P \in \mathcal{P}_L$ is equivalent to summing over all $x, z \in \mathbb{Z}_2^N$.

Expansion of the quantum state in the computational basis. We write the quantum state in the computational bitstring basis as

$$|\psi\rangle = \sum_{t \in \mathbb{Z}_2^N} \phi_t |t\rangle, \quad (3)$$

where $|t\rangle$ denotes the computational basis state labeled by the length- N bitstring $t = (t_1, \dots, t_N)$.

Action of Pauli operators on the computational basis. The actions of the Pauli operators X^x and Z^z on the computational basis are given by

$$X^x |t\rangle = |t \oplus x\rangle, \quad (4)$$

$$Z^z |t\rangle = (-1)^{z \cdot t} |t\rangle, \quad (5)$$

where \oplus denotes bitwise addition modulo 2, and $z \cdot t = \sum_{j=1}^N z_j t_j \pmod{2}$ is the binary inner product. Consequently,

$$P|\psi\rangle = \sum_t \phi_t (-1)^{z \cdot t} |t \oplus x\rangle. \quad (6)$$

Pauli expectation values and XOR-correlation structure. It then follows that

$$\langle \psi | P | \psi \rangle = \sum_t (-1)^{z \cdot t} \phi_{t \oplus x}^* \phi_t. \quad (7)$$

This expression exhibits an XOR-correlation structure, namely a weighted sum over correlations between the wavefunction amplitudes ϕ_t and their bit-shifted counterparts $\phi_{t \oplus x}$. In the following derivation, we first fix x and perform the summation over z .

Fourth-order modulus expansion and Walsh-Hadamard orthogonality. Define

$$g_x(t) := \phi_{t \oplus x}^* \phi_t, \quad (8)$$

and introduce

$$A(z) := \sum_{t \in \mathbb{Z}_2^N} (-1)^{z \cdot t} g_x(t), \quad (9)$$

so that

$$|A(z)|^4 = A(z)A^*(z)A(z)A^*(z). \quad (10)$$

Expanding this expression explicitly yields

$$|A(z)|^4 = \sum_{t_1, t_2, t_3, t_4} (-1)^{z \cdot (t_1 \oplus t_2 \oplus t_3 \oplus t_4)} \times g_x(t_1) g_x^*(t_2) g_x(t_3) g_x^*(t_4). \quad (11)$$

Since the definition of the SRE involves a sum over all $z \in \mathbb{Z}_2^N$, we can exploit the orthogonality relation of the Walsh-Hadamard transform defined on the group \mathbb{Z}_2^N ,

$$\sum_{z \in \mathbb{Z}_2^N} (-1)^{z \cdot s} = \begin{cases} 2^N, & s = 0, \\ 0, & s \neq 0, \end{cases} \quad (12)$$

to explicitly carry out the summation over z , obtaining

$$\sum_z |A(z)|^4 = 2^N \sum_{\substack{t_1, t_2, t_3, t_4 \\ t_1 \oplus t_2 \oplus t_3 \oplus t_4 = 0}} g_x(t_1) g_x^*(t_2) g_x(t_3) g_x^*(t_4). \quad (13)$$

The orthogonality of the Walsh-Hadamard transform projects the originally unconstrained fourfold sum onto the subspace satisfying $t_1 \oplus t_2 \oplus t_3 \oplus t_4 = 0$. This XOR constraint is the key to the subsequent efficient numerical implementation.

XOR-convolution structure and dimensionality reduction. The constraint $t_1 \oplus t_2 \oplus t_3 \oplus t_4 = 0$ allows one to eliminate one variable, for instance, by writing $t_4 = t_1 \oplus t_2 \oplus t_3$. Eq. (13) can thus be rewritten as

$$\sum_z |A(z)|^4 = 2^N \sum_{t_1, t_2, t_3} g_x(t_1) g_x^*(t_2) g_x(t_3) g_x^*(t_1 \oplus t_2 \oplus t_3). \quad (14)$$

The above triple sum has a characteristic XOR convolution structure (see Appendix A 3). To make this explicit, we introduce the intermediate function

$$C_x(s) := \sum_{t \in \mathbb{Z}_2^N} g_x(t) g_x^*(t \oplus s), \quad (15)$$

where $s \in \mathbb{Z}_2^N$.

Using Eq. (15) and appropriately relabeling the summation variables, Eq. (14) can be further simplified to

$$\begin{aligned} \sum_z |A(z)|^4 &= 2^N \sum_{s \in \mathbb{Z}_2^N} \left| \sum_{t \in \mathbb{Z}_2^N} g_x(t) g_x^*(t \oplus s) \right|^2 \\ &= 2^N \sum_{s \in \mathbb{Z}_2^N} |C_x(s)|^2. \end{aligned} \quad (16)$$

Exploiting properties of the WHT. We apply the WHT to $C_x(s)$, and define $G_x := \text{WHT}(g_x)$. Using property A 4, we obtain

$$\text{WHT}(C_x) = \sqrt{2^N} G_x \cdot G_x^* = \sqrt{2^N} |G_x|^2. \quad (17)$$

Applying the Parseval identity of the WHT A 5 to Eq. (16) yields

$$\sum_s |C_x(s)|^2 = \sum_k |\text{WHT}(C_x)(k)|^2. \quad (18)$$

This further leads to

$$\sum_s |C_x(s)|^2 = 2^N \sum_k |G_x(k)|^4. \quad (19)$$

Then we obtain (there is also a factor of 2^N in Eq. (16))

$$\sum_{P \in \mathcal{P}_L} |\langle \psi | P | \psi \rangle|^4 = 4^N \sum_{x, k} |\text{WHT}(\phi_{x \oplus k}^* \phi_x)|^4. \quad (20)$$

We note that the FWHT provides an efficient numerical implementation of the WHT. According to Appendix A 6, Eq. (20) can be rewritten as

$$\sum_{P \in \mathcal{P}_L} |\langle \psi | P | \psi \rangle|^4 = \sum_{x, k} |\text{FWHT}(\phi_{x \oplus k}^* \phi_x)|^4. \quad (21)$$

Final result. Therefore, Eq. (1) can be written as

$$\mathcal{M}_2(|\psi\rangle) = -\log \left(\frac{1}{d} \sum_{x, k} |\text{FWHT}(\phi_{x \oplus k}^* \phi_x)|^4 \right), \quad (22)$$

Eq. (22) is the final expression. In the next section, we will show how to use it to design Algorithm 1.

III. XOR-FWHT ALGORITHM FOR THE 2-SRES

By using Eq. (22), we design the Algorithm 1. It is worth emphasizing that the bitstrings x and k are represented by their integer encodings in the numerical implementation, which is straightforward for a computer to handle. The implementation requires performing d FWHTs, each of length d , leading to an overall time complexity of $O(2^N \times N2^N) = O(N4^N)$. The additional memory overhead originates from storing the reordered conjugate vector $\phi[x \oplus k]$ ($x = 0, \dots, d-1$); this overhead does not accumulate with k and is therefore acceptable. Moreover, the

computations corresponding to different values of k are mutually independent, making the algorithm naturally well-suited to parallel implementation. We provide implementation details in Python in Appendix B.

We benchmarked the performance of the algorithm on a workstation equipped with two Intel Xeon Platinum 8352V processors (36 cores per CPU, 72 cores in total). In the benchmarks, the input states were randomly generated Haar states obtained by normalizing complex Gaussian random vectors, and we measured the wall-clock time for a single evaluation of the 2-SRE. For different system sizes N , the typical runtimes are as follows: approximately 0.88 seconds for $N = 14$; about 12 seconds for $N = 16$; about 300 seconds for $N = 18$; and about 2 hours for $N = 20$. These numerical results are consistent with the theoretical time complexity $O(N4^N)$ of the algorithm.

Algorithm 1 XOR-FWHT Algorithm of the \mathcal{M}_2

Input: normalized state vector $\phi[0], \dots, \phi[d-1]$ in the computational basis, where $d = 2^N$.

Output: \mathcal{M}_2 .

```

1:  $r \leftarrow 0$ 
2:  $\mathbf{x} \leftarrow [0, 1, \dots, d-1]$ 
3: for  $k = 0$  to  $d-1$  do
4:   construct length- $d$  complex array  $G$  by

$$G[x] \leftarrow \overline{\psi[x \oplus k]} \psi[x] \quad (x = 0, \dots, d-1)$$

5:    $\hat{G} \leftarrow \text{FWHT}(G)$ 
6:    $r \leftarrow r + \sum_{u=0}^{d-1} |\hat{G}[u]|^4$ 
7: end for
8: return  $\mathcal{M}_2 \leftarrow -\log_2(r/d)$ 

```

IV. APPLICATIONS IN PHYSICAL EXAMPLES

In this section, we numerically present several representative physical examples by using algorithm 1 for evaluating 2-SRE.

A. Example 1. validation on Haar random states

First, we randomly sample Haar-random pure states from the Hilbert space according to the Haar measure. As typical quantum states, Haar-random states exhibit volume-law entanglement near the Page limit at the subsystem level, which causes tensor-network-based approaches to compute \mathcal{M}_2 to encounter an exponentially growing bond-dimension bottleneck as the system size increases. In contrast, the XOR-FWHT algorithm proposed in this work does not rely on the bond dimension of a tensor-network representation, but instead acts directly on the state vector itself, and therefore enables efficient evaluation of the magic measure \mathcal{M}_2 for Haar-random states.

As shown in Fig. 1(a), the numerical results are in good agreement with the theoretical prediction [164], thereby val-

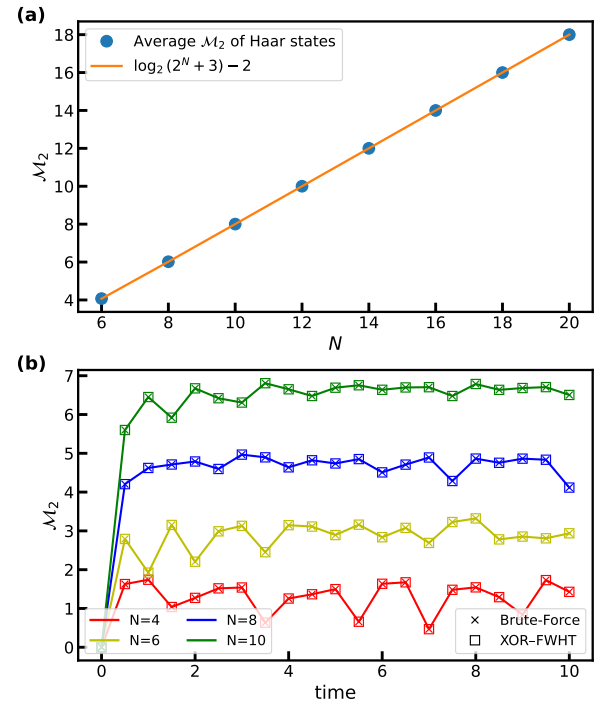


Figure 1. (a) The average 2-SRE \mathcal{M}_2 of Haar-random pure states as a function of the system size N . For each N , we independently sample 10–100 Haar-random states and compute the average. The solid line shows the theoretically predicted behavior $\log_2(2^N + 3) - 2$, which is in good agreement with the numerical results, indicating that \mathcal{M}_2 of Haar states grows approximately linearly with N . (b) Time evolution of \mathcal{M}_2 in the dynamics of the XXZ model, comparing results obtained from the brute-force approach and from the XOR-FWHT algorithm proposed in this work. The two methods yield identical numerical results throughout the entire time evolution, verifying the correctness and stability of the XOR-FWHT algorithm in dynamical calculations.

idating the correctness and applicability of the algorithm for highly entangled states.

B. Example 2. Hamiltonian quench dynamics

Next, we consider a one-dimensional XXZ spin- $\frac{1}{2}$ chain with the Hamiltonian

$$H_{\text{XXZ}} = \sum_{i=0}^{N-1} J (X_i X_{i+1} + Y_i Y_{i+1}) + \Delta Z_i Z_{i+1}, \quad (23)$$

where we set $J = 1$ and $\Delta = 0.5$ in the numerical calculations. We chose the Neél state $|\uparrow\downarrow\uparrow\downarrow\dots\rangle$ as the initial state and perform real-time evolution using exact diagonalization. At a series of discrete time points, we evaluate \mathcal{M}_2 of the evolved, as shown in Fig. 1(b). The figure also shows the nu-

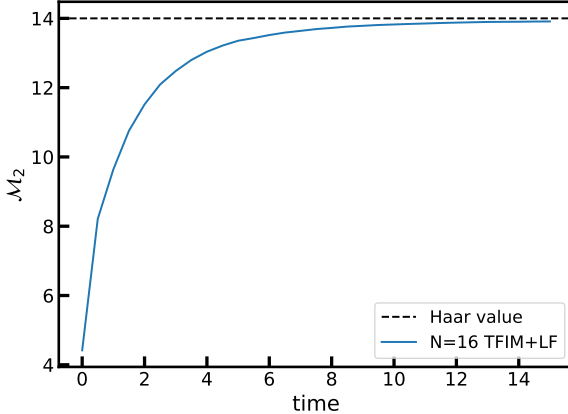


Figure 2. Time evolution of the 2-SRE \mathcal{M}_2 for $N = 16$ spins evolved under the TFIM with a longitudinal field. Starting from 100 random product states, $\mathcal{M}_2(t)$ rapidly grows and saturates at a value slightly below the Haar-random benchmark (dashed line) within the accessible time window.

numerical results for \mathcal{M}_2 obtained from both the brute-force approach and the XOR-FWHT algorithm proposed in this work. Throughout the time evolution, the results obtained by the two methods are in complete agreement within numerical precision. This agreement validates the correctness and reliability of the XOR-FWHT algorithm for time-evolved states. This result follows from our rigorous derivation rather than from any approximation or stochastic sampling, and therefore, the algorithm is numerically deterministic and exact.

We also consider the transverse-field Ising model with an additional longitudinal field (TFIM with longitudinal field), whose Hamiltonian is given by

$$H_{\text{TFIM+LF}} = -J \sum_{i=0}^{N-1} Z_i Z_{i+1} - h_x \sum_{i=0}^{N-1} X_i - h_z \sum_{i=0}^{N-1} Z_i, \quad (24)$$

where we set $J = 1$, $h_x = 1.5$, and $h_z = 1.5$, with the system size $N = 16$.

The initial state is chosen as a tensor product of random single-qubit states,

$$|\psi_0\rangle = \bigotimes_{i=1}^N \left(\cos \frac{\theta_i}{2} |\uparrow\rangle + e^{i\phi_i} \sin \frac{\theta_i}{2} |\downarrow\rangle \right), \quad (25)$$

where $\theta_i \in [0, \pi]$ and $\phi_i \in [0, 2\pi]$ are independent random variables. Although these initial states are unentangled, they are generally non-stabilizer states and thus carry local non-stabilizer resources. Starting from 100 different random initial states, we perform real-time evolution using the Krylov subspace method, and compute the SRE \mathcal{M}_2 during the evolution, followed by averaging over the results. The resulting dynamical behavior is shown in Fig. 2. We observe that, within the system size and time window considered, $\mathcal{M}_2(t)$ grows rapidly with time and gradually approaches saturation, while its value always remains slightly below the corresponding Haar-random-state benchmark. Notably, in Fig. 4(b) of

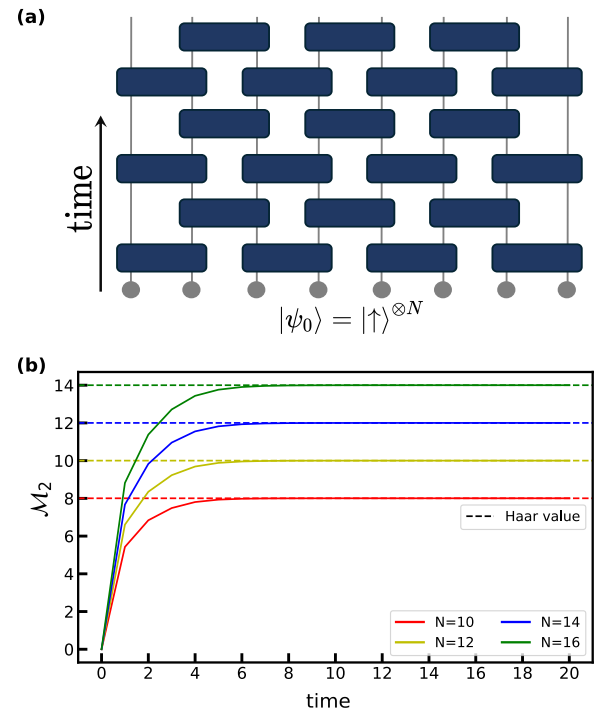


Figure 3. (a) Schematic of the 1D brickwork random circuit. The system is initialized in the product state $|\psi_0\rangle = |\uparrow\rangle^{\otimes N}$ and evolves under layers of nearest-neighbor Haar-random two-qubit gates. (b) Dynamics of the SRE \mathcal{M}_2 for system sizes $N = 10, 12, 14, 16$ with averaging 100 samples. The dashed horizontal lines indicate the theoretical saturation values corresponding to Haar-random states.

Ref. [165], this subtle deviation from the Haar value is not clearly resolved. We conjecture that this may be related to the intrinsic statistical errors of numerical evaluation methods based on finite sampling, which make it difficult to resolve such small deviations in \mathcal{M}_2 at that level of precision. In contrast, the exact XOR-FWHT algorithm employed in this work enables high-precision evaluation of \mathcal{M}_2 without resorting to stochastic sampling, thereby allowing such subtle but physically meaningful deviations to be clearly revealed. This provides a new numerical tool for further investigating the fine structure of magic resources in dynamical processes.

C. Example 3. random unitary circuit quench dynamics

Here, we consider a chain of N qubits with Hilbert space $\mathcal{H} = (\mathbb{C}^2)^{\otimes N}$ and initialize the system in the product state $|\psi_0\rangle = |\uparrow\rangle^{\otimes N}$. As shown in Fig. 3a, we build a 1D nearest-neighbor brickwork random circuit with open boundary conditions in which each blue brick is a two-qubit unitary acting on a neighboring pair $(i, i + 1)$ and is sampled independently from the Haar measure on $U(4)$. At discrete

time steps $t = 1, \dots, T$, one time step consists of an even-bond layer followed by an odd-bond layer. The even layer acts on $(0, 1), (2, 3), \dots, (N-2, N-1)$ and is denoted by $U_{\text{even}}^{(t)} = \prod_{k=0}^{\frac{N}{2}-1} U_{2k, 2k+1}^{(t)}$ with $U_{2k, 2k+1}^{(t)} \sim \text{Haar}(U(4))$. The odd layer acts on $(1, 2), (3, 4), \dots, (N-3, N-2)$ and is denoted by $U_{\text{odd}}^{(t)} = \prod_{k=0}^{\frac{N}{2}-2} V_{2k+1, 2k+2}^{(t)}$ with $V_{2k+1, 2k+2}^{(t)} \sim \text{Haar}(U(4))$. All two-qubit gates are sampled independently across bonds, layers, and time steps. The unitary for one time step is $U_t = U_{\text{odd}}^{(t)} U_{\text{even}}^{(t)}$, and the state evolves as $|\psi_t\rangle = U_t |\psi_{t-1}\rangle$. Equivalently, $|\psi_t\rangle = \left(\prod_{\tau=1}^t U_\tau \right) |\uparrow\rangle^{\otimes N}$. We record the full state at each time t .

As illustrated in Fig. 3b, we numerically simulated this setup using `TensorCircuit-NG` [166] for system sizes $N = 10, 12, 14, 16$. For all system sizes considered, the SRE dynamics saturates at long times to the corresponding Haar value.

V. CONCLUSION AND OUTLOOK

In this work, we propose a fast and exact algorithm for evaluating medium-scale 2-SRE \mathcal{M}_2 with a computational time complexity of $O(N4^N)$. Starting from the definition of \mathcal{M}_2 , we derive a fully deterministic reformulation based on XOR convolution and the WHT, without introducing any approximation, stochastic sampling, or additional assumptions on the structure of the quantum state throughout the derivation. The resulting expression can be efficiently implemented using the FWHT, leading to a substantial reduction in computational cost compared to brute-force approaches. We have made the complete algorithmic details and the corresponding Python implementation publicly available. Through several numerical examples, we demonstrate that our method accurately reproduces the theoretical expectation value of \mathcal{M}_2 for Haar-random states, and that it is in full numerical agreement with brute-force results for the system sizes where such comparisons are possible. More importantly, the algorithm achieves high numerical precision, allowing one to resolve small but physically meaningful deviations in \mathcal{M}_2 , thereby enabling the investigation of the fine structure of non-stabilizer resources in quantum states and dynamics.

Looking ahead, several promising directions remain for further exploration. One direct application of the present algorithm is the systematic study of the dynamical behavior of \mathcal{M}_2 in a variety of interacting quantum many-body models, as well as its interplay with other physical quantities such as entanglement and operator spreading. From a computational perspective, combining the current framework with tensor-network representations is particularly appealing, as this may further reduce the effective computational cost for large systems or weakly entangled states. More broadly, we expect that the algorithmic ideas developed in this work can serve as building blocks for the efficient evaluation of higher-order stabilizer Rényi entropies and related resource measures.

ACKNOWLEDGMENTS

J.-X. Zhong was supported by the National Natural Science Foundation of China (Grant Nos. 12374046 and 11874316), the Shanghai Science and Technology Innovation Action Plan (Grant No. 24LZ1400800), the National Basic Research Program of China (Grant No. 2015CB921103), and the Program for Changjiang Scholars and Innovative Research Teams in Universities (Grant No. IRT13093). H.-Z. Li is supported by a China Scholarship Council Scholarship.

Appendix A: Introduction to the WHT

To facilitate the reader's understanding of the logical structure of the derivations presented in the main text, we summarize in this appendix the properties and features of the WHT used in this work.

1. Definition

We first define the WHT of a function $f : \{0, 1\}^N \rightarrow \mathbb{C}$ as

$$\hat{f}(k) = \frac{1}{\sqrt{2^N}} \sum_{x \in \{0, 1\}^N} (-1)^{k \cdot x} f(x), \quad (\text{A1})$$

where $k \cdot x$ denotes the mod-2 inner product.

2. Property of Involution and Inverse Transform

The WHT satisfies

$$\text{WHT}(\text{WHT}(f)) = f. \quad (\text{A2})$$

Therefore, the inverse transform is given by

$$\text{IWHT}(f) = \text{WHT}(f). \quad (\text{A3})$$

3. Properties of XOR-Convolution Theorem

We define the XOR convolution as

$$(f *_{\oplus} g)(x) = \sum_{y \in \mathbb{Z}_2^N} f(y) g(x \oplus y), \quad (\text{A4})$$

then

$$\text{WHT}(f *_{\oplus} g) = \sqrt{2^N} \text{WHT}(f) \cdot \text{WHT}(g), \quad (\text{A5})$$

where the symbol \cdot on the right-hand side denotes pointwise multiplication of vectors.

4. Property I: Compatibility with Complex Conjugation

For any complex-valued vector f , one has

$$\text{WHT}(f^*)(k) = (\text{WHT}(f)(k))^*. \quad (\text{A6})$$

Consequently, $\text{WHT}(f) \text{WHT}(f^*) = |\text{WHT}(f)|^2$.

5. Property II: Parseval's Theorem

The WHT preserves the ℓ_2 norm:

$$\sum_{x \in \mathbb{Z}_2^N} |f(x)|^2 = \sum_{k \in \mathbb{Z}_2^N} |\text{WHT}(f)(k)|^2. \quad (\text{A7})$$

6. Numerical Algorithm of FWTH

The WHT admits an efficient numerical implementation known as the FWHT. Rather than defining a new transform, the FWHT computes the WHT by exploiting the recursive structure of the Hadamard matrix. In our implementation, the FWHT evaluates the unnormalized transform, which is related to the normalized WHT by

$$\text{FWHT}(f) = \sqrt{2^N} \text{WHT}(f). \quad (\text{A8})$$

Concretely, the FWHT proceeds via iterative butterfly updates of the form

$$(a, b) \mapsto (a + b, a - b), \quad (\text{A9})$$

applied recursively over N levels for functions defined on $\{0, 1\}^N$, resulting in an overall computational complexity

of $O(N2^N)$. Implementation details are provided in Appendix B.

Appendix B: Python Implementation of Algorithm 1

```

1 import numpy as np
2
3 def FWHT_inplace(a):
4     n = a.shape[0]
5     h = 1
6     while h < n:
7         for i in range(0, n, 2*h):
8             u = a[i:i+h]
9             v = a[i+h:i+2*h]
10            u[:, :], v[:, :] = u+v, u-v
11            h *= 2
12
13 def M_func(psi):
14     d = psi.shape[0]
15     x = np.arange(d, dtype=np.int64)
16     total = 0.0
17     for k in range(d):
18         A = np.conjugate(psi[x^k]) * psi
19         FWHT_inplace(A)
20         total += (np.sum(np.abs(A) ** 4))
21
22 return -np.log2(total/d)

```

It should be emphasized that, in the practical implementation of this code, we also employ JIT and parallelization techniques, enabling us to fully utilize multicore CPU resources.

[1] E. Chitambar and G. Gour, Quantum resource theories, *Rev. Mod. Phys.* **91**, 025001 (2019).

[2] P. W. Shor, Polynomial-time algorithms for prime factorization and discrete logarithms on a quantum computer, *SIAM Journal on Computing* **26**, 1484 (1997).

[3] M. A. Nielsen and I. L. Chuang, *Quantum Computation and Quantum Information: 10th Anniversary Edition* (Cambridge University Press, 2010).

[4] A. J. Daley, I. Bloch, C. Kokail, S. Flannigan, N. Pearson, M. Troyer, and P. Zoller, Practical quantum advantage in quantum simulation, *Nature* **607**, 667 (2022).

[5] H.-Y. Huang, S. Choi, J. R. McClean, and J. Preskill, The vast world of quantum advantage, [arXiv:2508.05720](https://arxiv.org/abs/2508.05720) (2025).

[6] O. Lanes, M. Beji, A. D. Corcoles, C. Dalyac, J. M. Gambetta, L. Henriet, A. Javadi-Abhari, A. Kandala, A. Mezzacapo, C. Porter, S. Sheldon, J. Watrous, C. Zoufal, A. Dauphin, and B. Peropadre, A framework for quantum advantage, [arXiv:2506.20658](https://arxiv.org/abs/2506.20658) (2025).

[7] L. Amico, R. Fazio, A. Osterloh, and V. Vedral, Entanglement in many-body systems, *Rev. Mod. Phys.* **80**, 517 (2008).

[8] R. Horodecki, P. Horodecki, M. Horodecki, and K. Horodecki, Quantum entanglement, *Rev. Mod. Phys.* **81**, 865 (2009).

[9] E. Chitambar and G. Gour, Quantum resource theories, *Rev. Mod. Phys.* **91**, 025001 (2019).

[10] Z.-W. Liu and A. Winter, Many-body quantum magic, *PRX Quantum* **3**, 020333 (2022).

[11] L. Leone, S. F. E. Oliviero, and A. Hamma, Stabilizer Rényi entropy, *Phys. Rev. Lett.* **128**, 050402 (2022).

[12] L. Leone and L. Bittel, Stabilizer entropies are monotones for magic-state resource theory, *Phys. Rev. A* **110**, L040403 (2024).

[13] E. Tirrito, P. S. Tarabunga, G. Lami, T. Chanda, L. Leone, S. F. E. Oliviero, M. Dalmonte, M. Collura, and A. Hamma, Quantifying nonstabilizer entropy through entanglement spectrum flatness, *Phys. Rev. A* **109**, L040401 (2024).

[14] X. Turkeshi, M. Schirò, and P. Sierant, Measuring nonstabilizer entropy via multifractal flatness, *Phys. Rev. A* **108**, 042408 (2023).

[15] X. Turkeshi, A. Dymarsky, and P. Sierant, Pauli spectrum and nonstabilizer entropy of typical quantum many-body states, *Phys. Rev. B* **111**, 054301 (2025).

[16] X. Turkeshi, E. Tirrito, and P. Sierant, Magic spreading in random quantum circuits, *Nat. Commun.* **16**, 2575 (2025).

[17] B. Jasser, J. Odavić, and A. Hamma, Stabilizer entropy and entanglement complexity in the Sachdev-Ye-Kitaev model, [arXiv:2502.03093](https://arxiv.org/abs/2502.03093) (2025).

[18] M. Viscardi, M. Dalmonte, A. Hamma, and E. Tirrito, Interplay of entanglement structures and stabilizer entropy in spin models, [arXiv:2503.08620](https://arxiv.org/abs/2503.08620) (2025).

[19] D. Iannotti, G. Esposito, L. Campos Venuti, and A. Hamma, Entanglement and Stabilizer entropies of random bipartite pure quantum states, *Quantum* **9**, 1797 (2025).

[20] S. Cusumano, L. C. Venuti, S. Cepollaro, G. Esposito, D. Iannotti, B. Jasser, J. O. c, M. Viscardi, and A. Hamma, Non-stabilizerness and violations of chsh inequalities, [arXiv:2504.03351](https://arxiv.org/abs/2504.03351) (2025).

[21] L. Bittel and L. Leone, Operational interpretation of the stabilizer entropy, [arXiv:2507.22883](https://arxiv.org/abs/2507.22883) (2025).

[22] N. D. Varikuti, S. Bandyopadhyay, and P. Hauke, Impact of clifford operations on non-stabilizing power and quantum chaos, [arXiv:2505.14793](https://arxiv.org/abs/2505.14793) (2025).

[23] E. Tirrito, X. Turkeshi, and P. Sierant, Anticoncentration and nonstabilizerness spreading under ergodic quantum dynamics, [arXiv:2412.10229](https://arxiv.org/abs/2412.10229) (2025).

[24] P. Zhang, S. Zhou, and N. Sun, Stabilizer rényi entropy and its transition in the coupled sachdev-ye-kitaev model, [arXiv:2509.17417](https://arxiv.org/abs/2509.17417) (2025).

[25] D. Qian and J. Wang, Quantum nonlocal nonstabilizerness, *Phys. Rev. A* **111**, 052443 (2025).

[26] C. P. Moca, D. Sticlet, B. Dóra, A. Valli, D. Szombathy, and G. Zaránd, Non-stabilizerness generation in a multi-particle quantum walk, [arXiv:2504.19750](https://arxiv.org/abs/2504.19750) (2025).

[27] N. Dowling, P. Kos, and X. Turkeshi, Magic resources of the heisenberg picture, *Phys. Rev. Lett.* **135**, 050401 (2025).

[28] S. Bera and M. Schirò, Non-stabilizerness of sachdev-ye-kitaev model, [arXiv:2502.01582](https://arxiv.org/abs/2502.01582) (2025).

[29] S. Masot-Llima and A. Garcia-Saez, Stabilizer tensor networks: Universal quantum simulator on a basis of stabilizer states, *Phys. Rev. Lett.* **133**, 230601 (2024).

[30] S. Aditya, A. Summer, P. Sierant, and X. Turkeshi, Mpemba effects in quantum complexity, [arXiv:2509.22176](https://arxiv.org/abs/2509.22176) (2025).

[31] T. Hernández-Yanes, P. Sierant, J. Zakrzewski, and M. Płodzień, Non-stabilizerness in quantum-enhanced metrological protocols, [arXiv:2510.01380](https://arxiv.org/abs/2510.01380) (2025).

[32] P. R. N. Falcão, P. Sierant, J. Zakrzewski, and E. Tirrito, Magic dynamics in many-body localized systems, [arXiv:2503.07468](https://arxiv.org/abs/2503.07468) (2025).

[33] D. Sticlet, B. Dóra, D. Szombathy, G. Zaránd, and C. P. Moca, Non-stabilizerness in open XXZ spin chains: Universal scaling and dynamics, [arXiv:2504.11139](https://arxiv.org/abs/2504.11139) (2025).

[34] E. Tirrito, P. S. Tarabunga, D. S. Bhakuni, M. Dalmonte, P. Sierant, and X. Turkeshi, Universal spreading of nonstabilizerness and quantum transport, [arXiv:2506.12133](https://arxiv.org/abs/2506.12133) (2025).

[35] Y. Zhang and Y. Gu, Quantum magic dynamics in random circuits, [arXiv:2410.21128](https://arxiv.org/abs/2410.21128) (2024).

[36] C. Cao, G. Cheng, A. Hamma, L. Leone, W. Munizzi, and S. F. E. Oliviero, Gravitational back-reaction is magical, [arXiv:2403.07056](https://arxiv.org/abs/2403.07056) (2025).

[37] P. S. Tarabunga and C. Castelnovo, Magic in generalized rokhsar-kivelson wavefunctions, *Quantum* **8**, 1347 (2024).

[38] X. Qian, J. Huang, and M. Qin, Augmenting a finite-temperature tensor network with clifford circuits, *Phys. Rev. B* **112**, 115150 (2025).

[39] X. Qian, J. Huang, and M. Qin, Clifford circuits augmented time-dependent variational principle, *Phys. Rev. Lett.* **134**, 150404 (2025).

[40] J. Huang, X. Qian, and M. Qin, Nonstabilizerness entanglement entropy: A measure of hardness in the classical simulation of quantum many-body systems with tensor network states, *Phys. Rev. A* **112**, 012425 (2025).

[41] X. Qian, J. Huang, and M. Qin, Augmenting density matrix renormalization group with clifford circuits, *Phys. Rev. Lett.* **133**, 190402 (2024).

[42] M. Frau, P. S. Tarabunga, M. Collura, E. Tirrito, and M. Dalmonte, Stabilizer disentangling of conformal field theories, *SciPost Phys.* **18**, 165 (2025).

[43] C. Fan, X. Qian, H.-C. Zhang, R.-Z. Huang, M. Qin, and T. Xiang, Disentangling critical quantum spin chains with clifford circuits, *Phys. Rev. B* **111**, 085121 (2025).

[44] J. Huang, X. Qian, and M. Qin, Clifford circuits augmented matrix product states for fermion systems, [arXiv:2501.00413](https://arxiv.org/abs/2501.00413) (2024).

[45] Y.-M. Ding, Z. Wang, and Z. Yan, Evaluating many-body stabilizer rényi entropy by sampling reduced pauli strings: Singularities, volume law, and nonlocal magic, *PRX Quantum* **6**, 030328 (2025).

[46] D. A. Korbany, M. J. Gullans, and L. Piroli, Long-range nonstabilizerness and phases of matter, [arXiv:2502.19504](https://arxiv.org/abs/2502.19504) (2025).

[47] F. Wei and Z.-W. Liu, Long-range nonstabilizerness from quantum codes, orders, and correlations, [arXiv:2503.04566](https://arxiv.org/abs/2503.04566) (2025).

[48] P. S. Tarabunga and T. Haug, Efficient mutual magic and magic capacity with matrix product states, [arXiv:2504.07230](https://arxiv.org/abs/2504.07230) (2025).

[49] D. Szombathy, A. Valli, C. P. Moca, L. Farkas, and G. Zaránd, Independent stabilizer rényi entropy and entanglement fluctuations in random unitary circuits, [arXiv:2501.11489](https://arxiv.org/abs/2501.11489) (2025).

[50] Z.-Y. Hou, C. Cao, and Z.-C. Yang, Stabilizer entanglement enhances magic injection, [arXiv:2503.20873](https://arxiv.org/abs/2503.20873) (2025).

[51] M. Hoshino, M. Oshikawa, and Y. Ashida, Stabilizer rényi entropy and conformal field theory, [arXiv:2503.13599](https://arxiv.org/abs/2503.13599) (2025).

[52] P. S. Tarabunga and E. Tirrito, Magic transition in measurement-only circuits, [arXiv:2407.15939](https://arxiv.org/abs/2407.15939) (2024).

[53] E. Tirrito, L. Lumia, A. Paviglianiti, G. Lami, A. Silva, X. Turkeshi, and M. Collura, Magic phase transitions in monitored gaussian fermions, [arXiv:2507.07179](https://arxiv.org/abs/2507.07179) (2025).

[54] C. Wang, Z.-C. Yang, T. Zhou, and X. Chen, Magic transition in monitored free fermion dynamics, [arXiv:2507.10688](https://arxiv.org/abs/2507.10688) (2025).

[55] G. C. Santra, A. Windey, S. Bandyopadhyay, A. Legramandi, and P. Hauke, Complexity transitions in chaotic quantum systems, [arXiv:2505.09707](https://arxiv.org/abs/2505.09707) (2025).

[56] T. Haug, L. Aolita, and M. Kim, Probing quantum complexity via universal saturation of stabilizer entropies, *Quantum* **9**, 1801 (2025).

[57] T. Haug and L. Piroli, Stabilizer entropies and nonstabilizerness monotones, *Quantum* **7**, 1092 (2023).

[58] T. Haug and L. Piroli, Quantifying nonstabilizerness of matrix product states, *Phys. Rev. B* **107**, 035148 (2023).

[59] G. Lami and M. Collura, Nonstabilizerness via Perfect Pauli Sampling of Matrix Product States, *Phys. Rev. Lett.* **131**, 180401 (2023).

[60] G. Lami and M. Collura, Unveiling the Stabilizer Group of a Matrix Product State, *Phys. Rev. Lett.* **133**, 010602 (2024).

[61] P. S. Tarabunga, E. Tirrito, T. Chanda, and M. Dalmonte, Many-body magic via pauli-markov chains—from criticality to gauge theories, *PRX Quantum* **4**, 040317 (2023).

[62] P. S. Tarabunga, E. Tirrito, M. C. Bañuls, and M. Dalmonte, Nonstabilizerness via matrix product states in the pauli basis, *Phys. Rev. Lett.* **133**, 010601 (2024).

[63] M. Van den Nest, Universal quantum computation with little entanglement, *Phys. Rev. Lett.* **110**, 060504 (2013).

[64] N. Schuch, M. M. Wolf, F. Verstraete, and J. I. Cirac, Entropy scaling and simulability by matrix product states, *Phys. Rev. Lett.* **100**, 030504 (2008).

[65] G. Vidal, Efficient classical simulation of slightly entangled quantum computations, *Phys. Rev. Lett.* **91**, 147902 (2003).

[66] G. Vidal, Efficient simulation of one-dimensional quantum many-body systems, *Phys. Rev. Lett.* **93**, 040502 (2004).

[67] M. Oszmaniec, N. Dangniam, M. E. Morales, and Z. Zim-

borás, Fermion sampling: A robust quantum computational advantage scheme using fermionic linear optics and magic input states, *PRX Quantum* **3**, 020328 (2022).

[68] D. Gottesman, The heisenberg representation of quantum computers, [arXiv:quant-ph/9807006](https://arxiv.org/abs/quant-ph/9807006) (1998).

[69] S. Aaronson and D. Gottesman, Improved simulation of stabilizer circuits, *Phys. Rev. A* **70**, 052328 (2004).

[70] J. Preskill, Quantum computing in the NISQ era and beyond, *Quantum* **2**, 79 (2018).

[71] Z.-W. Liu and A. Winter, Many-body quantum magic, *PRX Quantum* **3**, 020333 (2022).

[72] L. Daguerre, R. Blume-Kohout, N. C. Brown, D. Hayes, and I. H. Kim, Experimental demonstration of high-fidelity logical magic states from code switching, *Phys. Rev. X* **15**, 041008 (2025).

[73] D. Aasen, M. Aghaee, Z. Alam, M. Andrzejczuk, A. Antipov, M. Astafev, L. Avilovas, A. Barzegar, B. Bauer, J. Becker, J. M. Bello-Rivas, U. Bhaskar, A. Bocharov, S. Boddapati, D. Bohn, *et al.*, Roadmap to fault tolerant quantum computation using topological qubit arrays, [arXiv:2502.12252](https://arxiv.org/abs/2502.12252) (2025).

[74] T. Peham, L. Schmid, L. Berent, M. Müller, and R. Wille, Automated synthesis of fault-tolerant state preparation circuits for quantum error-correction codes, *PRX Quantum* **6**, 020330 (2025).

[75] P. Hayden and J. Preskill, Black holes as mirrors: quantum information in random subsystems, *Journal of High Energy Physics* **2007**, 120 (2007).

[76] Y. Sekino and L. Susskind, Fast scramblers, *Journal of High Energy Physics* **2008**, 065 (2008).

[77] P. Hosur, X.-L. Qi, D. A. Roberts, and B. Yoshida, Chaos in quantum channels, *Journal of High Energy Physics* **2016**, 004 (2016).

[78] C. W. von Keyserlingk, T. Rakovszky, F. Pollmann, and S. L. Sondhi, Operator hydrodynamics, OTOCs, and entanglement growth in systems without conservation laws, *Physical Review X* **8**, 021013 (2018).

[79] V. Khemani, A. Vishwanath, and D. A. Huse, Operator spreading and the emergence of dissipative hydrodynamics under unitary evolution with conservation laws, *Physical Review X* **8**, 031057 (2018).

[80] B. Swingle, Unscrambling the physics of out-of-time-order correlators, *Nature Physics* **14**, 988 (2018).

[81] S. Liu, H.-K. Zhang, S. Yin, and S.-X. Zhang, Symmetry restoration and quantum mpemba effect in symmetric random circuits, *Physical Review Letters* **133**, 140405 (2024).

[82] S. Liu, H.-K. Zhang, S. Yin, S.-X. Zhang, and H. Yao, Symmetry restoration and quantum mpemba effect in many-body localization systems, *Science Bulletin* **70**, 3991–3996 (2025).

[83] H. Yu, Z.-X. Li, and S.-X. Zhang, Symmetry breaking dynamics in quantum many-body systems, *Chinese Physics Letters* **42**, 110602 (2025).

[84] K. Huang, X. Li, D. A. Huse, and A. Chan, Out-of-time-order correlations and quantum chaos, *Scholarpedia* **18**, 55237 (2023).

[85] C. Liu and W. W. Ho, Solvable entanglement dynamics in quantum circuits with generalized space-time duality, *Phys. Rev. Res.* **7**, L012011 (2025).

[86] Y.-Q. Chen, S. Liu, and S.-X. Zhang, Subsystem Information Capacity in Random Circuits and Hamiltonian Dynamics, *Quantum* **9**, 1783 (2025).

[87] S. Liu, M.-R. Li, S.-X. Zhang, S.-K. Jian, and H. Yao, Noise-induced phase transitions in hybrid quantum circuits, *Phys. Rev. B* **110**, 064323 (2024).

[88] S. Liu, M.-R. Li, S.-X. Zhang, and S.-K. Jian, Entanglement structure and information protection in noisy hybrid quantum circuits, *Phys. Rev. Lett.* **132**, 240402 (2024).

[89] S. F. E. Oliviero, L. Leone, and A. Hamma, Magic-state resource theory for the ground state of the transverse-field ising model, *Phys. Rev. A* **106**, 042426 (2022).

[90] P. S. Tarabunga, Critical behaviors of non-stabilizerness in quantum spin chains, *Quantum* **8**, 1413 (2024).

[91] D. Rattacaso, L. Leone, S. F. E. Oliviero, and A. Hamma, Stabilizer entropy dynamics after a quantum quench, *Phys. Rev. A* **108**, 042407 (2023).

[92] G. Passarelli, R. Fazio, and P. Lucignano, Nonstabilizerness of permutationally invariant systems, *Phys. Rev. A* **110**, 022436 (2024).

[93] G. Passarelli, P. Lucignano, D. Rossini, and A. Russomanno, Chaos and magic in the dissipative quantum kicked top, *Quantum* **9**, 1653 (2025).

[94] M. Frau, P. S. Tarabunga, M. Collura, M. Dalmonte, and E. Tirrito, Nonstabilizerness versus entanglement in matrix product states, *Phys. Rev. B* **110**, 045101 (2024).

[95] J. C. M. de la Fuente, T. D. Ellison, M. Cheng, and D. J. Williamson, Topological stabilizer models on continuous variables, [arXiv:2411.04993](https://arxiv.org/abs/2411.04993) (2025).

[96] P. S. Tarabunga, E. Tirrito, T. Chanda, and M. Dalmonte, Many-body magic via pauli-markov chains—from criticality to gauge theories, *PRX Quantum* **4**, 040317 (2023).

[97] P. R. N. Falcão, P. S. Tarabunga, M. Frau, E. Tirrito, J. Zakrzewski, and M. Dalmonte, Nonstabilizerness in u(1) lattice gauge theory, *Phys. Rev. B* **111**, L081102 (2025).

[98] M. Frau, P. S. Tarabunga, M. Collura, E. Tirrito, and M. Dalmonte, Stabilizer disentangling of conformal field theories, *SciPost Phys.* **18**, 165 (2025).

[99] A. Paviglianiti, G. Lami, M. Collura, and A. Silva, Estimating nonstabilizerness dynamics without simulating it, *PRX Quantum* **6**, 030320 (2025).

[100] M. Bejan, C. McLauchlan, and B. Béri, Dynamical magic transitions in monitored clifford+*t* circuits, *PRX Quantum* **5**, 030332 (2024).

[101] H.-Z. Li, Y.-R. Zhang, Y.-J. Zhao, X. Huang, and J.-X. Zhong, Nonstabilizerness in stark many-body localization, [arXiv:2512.16859](https://arxiv.org/abs/2512.16859) (2025).

[102] P. R. N. Falcão, P. Sierant, J. Zakrzewski, and E. Tirrito, Nonstabilizerness dynamics in many-body localized systems, *Phys. Rev. Lett.* **135**, 240404 (2025).

[103] E. Tirrito, X. Turkeshi, and P. Sierant, Anticoncentration and nonstabilizerness spreading under ergodic quantum dynamics, *Phys. Rev. Lett.* **135**, 220401 (2025).

[104] A. I. Larkin and Y. N. Ovchinnikov, Quasiclassical method in the theory of superconductivity, *Soviet Physics JETP* **28**, 1200 (1969).

[105] S. H. Shenker and D. Stanford, Black holes and the butterfly effect, *Journal of High Energy Physics* **2014**, 067 (2014).

[106] J. Maldacena, S. H. Shenker, and D. Stanford, A bound on chaos, *Journal of High Energy Physics* **2016**, 106 (2016).

[107] K. Hashimoto, K. Murata, and R. Yoshii, Out-of-time-order correlators in quantum mechanics, *Journal of High Energy Physics* **2017**, 138 (2017).

[108] D. A. Roberts and B. Yoshida, Chaos and complexity by design, *Journal of High Energy Physics* **2017**, 121 (2017).

[109] J. Cotler, N. Hunter-Jones, J. Liu, and B. Yoshida, Chaos, complexity, and random matrices, *Journal of High Energy Physics* **2017**, 048 (2017).

[110] L. Leone, S. F. E. Oliviero, Y. Zhou, and A. Hamma, Quantum chaos is quantum, *Quantum* **5**, 453 (2021).

[111] K. Goto, T. Nosaka, and M. Nozaki, Probing chaos by magic

monotones, *Physical Review D* **106**, 126009 (2022).

[112] T. Prosen, Many-body quantum chaos and dual-unitarity round-a-face, *Chaos* **31**, 093101 (2021).

[113] S. Maity and R. Hamazaki, Local spreading of stabilizer rényi entropy in a brickwork random clifford circuit, [arXiv:2511.07769](https://arxiv.org/abs/2511.07769) (2025).

[114] S. Aditya, X. Turkeshi, and P. Sierant, Growth and spreading of quantum resources under random circuit dynamics, [arXiv:2512.14827](https://arxiv.org/abs/2512.14827) (2025).

[115] H.-Z. Li, J.-X. Zhong, and X.-J. Yu, Measurement-induced entanglement phase transition in free fermion systems, *Journal of Physics: Condensed Matter* **37**, 273002 (2025).

[116] H.-Z. Li, M. Wan, and J.-X. Zhong, Fate of non-hermitian free fermions with wannier-stark ladder, *Phys. Rev. B* **110**, 094310 (2024).

[117] W. Wang, H.-Z. Li, and J.-X. Zhong, Non-hermitian many-body localization in asymmetric chains with long-range interaction, [arXiv:2510.08277](https://arxiv.org/abs/2510.08277) (2025).

[118] X. Huang, H.-Z. Li, Y.-J. Zhao, S. Liu, and J.-X. Zhong, Quantum feedback induced entanglement relaxation and dynamical phase transition in monitored free fermion chains with a wannier-stark ladder, *Phys. Rev. B* **111**, 184302 (2025).

[119] Y.-J. Zhao, X. Huang, Y.-R. Zhang, H.-Z. Li, and J.-X. Zhong, Entanglement phases and phase transitions in monitored free fermion system due to localizations, [arXiv:2509.09538](https://arxiv.org/abs/2509.09538) (2025).

[120] H.-L. Zhang, H.-Z. Li, S. Yang, and X.-J. Yu, Quantum phase transition and critical behavior between the gapless topological phases, *Phys. Rev. A* **109**, 062226 (2024).

[121] H.-Z. Li, C. H. Lee, S. Liu, S.-X. Zhang, and J.-X. Zhong, Quantum mpemba effect in long-ranged u(1)-symmetric random circuits, [arXiv:2512.06775](https://arxiv.org/abs/2512.06775) (2025).

[122] S.-X. Zhang and H. Yao, Universal properties of many-body localization transitions in quasiperiodic systems, *Phys. Rev. Lett.* **121**, 206601 (2018).

[123] S. Liu, S.-X. Zhang, C.-Y. Hsieh, S. Zhang, and H. Yao, Discrete time crystal enabled by stark many-body localization, *Phys. Rev. Lett.* **130**, 120403 (2023).

[124] S. Liu, S.-X. Zhang, C.-Y. Hsieh, S. Zhang, and H. Yao, Probing many-body localization by excited-state variational quantum eigensolver, *Phys. Rev. B* **107**, 024204 (2023).

[125] S. Liu, H.-K. Zhang, S. Yin, S.-X. Zhang, and H. Yao, Symmetry restoration and quantum mpemba effect in many-body localization systems, *Science Bulletin* **70**, 3991 (2025).

[126] S. Liu, S.-K. Jian, and S.-X. Zhang, Noisy monitored quantum circuits, [arXiv:2512.18783](https://arxiv.org/abs/2512.18783) (2025).

[127] S. Liu, Z. Wu, S.-X. Zhang, and H. Yao, Supersymmetry dynamics on rydberg atom arrays, *Phys. Rev. B* **112**, L020301 (2025).

[128] X.-J. Yu, S. Yang, S. Liu, H.-Q. Lin, and S.-K. Jian, Gapless symmetry-protected topological states in measurement-only circuits, [arXiv:2501.03851](https://arxiv.org/abs/2501.03851) (2025).

[129] J. M. Koh, T. Tai, Y. H. Phee, W. E. Ng, and C. H. Lee, Stabilizing multiple topological fermions on a quantum computer, *npj Quantum Information* **8**, 16 (2022).

[130] J. M. Koh, T. Tai, and C. H. Lee, Realization of higher-order topological lattices on a quantum computer, *Nature Communications* **15**, 5807 (2024).

[131] T. Chen, R. Shen, C. H. Lee, and B. Yang, High-fidelity realization of the AKLT state on a NISQ-era quantum processor, *SciPost Phys.* **15**, 170 (2023).

[132] R. Shen, T. Chen, B. Yang, Y. Zhong, and C. H. Lee, Robust simulations of many-body symmetry-protected topological phase transitions on a quantum processor, [arXiv:2503.08776](https://arxiv.org/abs/2503.08776) (2025).

[133] S. Miyashita, T. Satoh, M. Sugawara, N. Benchasattabuse, K. M. Nakanishi, M. Hajdušek, H. Choi, and R. V. Meter, Digital quantum simulator for the time-dependent dirac equation using discrete-time quantum walks, [arXiv:2305.19568](https://arxiv.org/abs/2305.19568) (2023).

[134] N. K. Mohan, R. Bhowmick, D. Kumar, and R. Chaurasiya, Digital quantum simulations of hong-ou-mandel interference, [arXiv:2402.17522](https://arxiv.org/abs/2402.17522) (2024).

[135] B. Fauseweh, Quantum many-body simulations on digital quantum computers: State-of-the-art and future challenges, *Nat. Commun.* **15**, 2123 (2024).

[136] V. Veitch, S. A. Hamed Mousavian, D. Gottesman, and J. Emerson, The resource theory of stabilizer quantum computation, *New Journal of Physics* **16**, 013009 (2014).

[137] W. K. Wootters, A wigner-function formulation of finite-state quantum mechanics, *Annals of Physics* **176**, 1 (1987).

[138] V. Veitch, C. Ferrie, D. Gross, and J. Emerson, Negative quasi-probability as a resource for quantum computation, *New Journal of Physics* **14**, 113011 (2012).

[139] S. Bravyi and D. Gosset, Improved classical simulation of quantum circuits dominated by clifford gates, *Phys. Rev. Lett.* **116**, 250501 (2016).

[140] S. Bravyi, G. Smith, and J. A. Smolin, Trading classical and quantum computational resources, *Phys. Rev. X* **6**, 021043 (2016).

[141] X. Wang, M. M. Wilde, and Y. Su, Efficiently computable bounds for magic state distillation, *Phys. Rev. Lett.* **124**, 090505 (2020).

[142] A. Heimendahl, F. Montealegre-Mora, F. Vallentin, and D. Gross, Stabilizer extent is not multiplicative, *Quantum* **5**, 400 (2021).

[143] L. Leone, S. F. E. Oliviero, and A. Hamma, Nonstabilizerness determining the hardness of direct fidelity estimation, *Phys. Rev. A* **107**, 022429 (2023).

[144] L. Leone and L. Bittel, Stabilizer entropies are monotones for magic-state resource theory, *Phys. Rev. A* **110**, L040403 (2024).

[145] T. Haug and L. Piroli, Quantifying nonstabilizerness of matrix product states, *Phys. Rev. B* **107**, 035148 (2023).

[146] G. Lami and M. Collura, Nonstabilizerness via perfect pauli sampling of matrix product states, *Phys. Rev. Lett.* **131**, 180401 (2023).

[147] P. S. Tarabunga, E. Tirrito, M. C. Bañuls, and M. Dalmonte, Nonstabilizerness via matrix product states in the pauli basis, *Phys. Rev. Lett.* **133**, 010601 (2024).

[148] G. Lami and M. Collura, Unveiling the stabilizer group of a matrix product state, *Phys. Rev. Lett.* **133**, 010602 (2024).

[149] C. Cao, M. J. Gullans, B. Lackey, and Z. Wang, Quantum lego expansion pack: Enumerators from tensor networks, *PRX Quantum* **5**, 030313 (2024).

[150] L.-Y.-N. Liu, S. Yi, and J. Cui, Stabilizer rényi entropy for translation-invariant matrix product states, [arXiv:2508.03534](https://arxiv.org/abs/2508.03534) (2025).

[151] G. Lami, T. Haug, and J. De Nardis, Quantum state designs with clifford-enhanced matrix product states, *PRX Quantum* **6**, 010345 (2025).

[152] M. Hoshino and Y. Ashida, Stabilizer rényi entropy encodes fusion rules of topological defects and boundaries, [arXiv:2507.10656](https://arxiv.org/abs/2507.10656) (2025).

[153] L. Chen, R. J. Garcia, K. Bu, and A. Jaffe, Magic of random matrix product states, *Phys. Rev. B* **109**, 174207 (2024).

[154] Z. Liu and B. K. Clark, Nonequilibrium quantum monte carlo algorithm for stabilizer rényi entropy in spin systems, *Phys.*

Rev. B **111**, 085144 (2025).

[155] P. S. Tarabunga and C. Castelnovo, Magic in generalized Rokhsar-Kivelson wavefunctions, *Quantum* **8**, 1347 (2024).

[156] S. Crew and H. H. Lu, Learning magic in the schwinger model, [arXiv:2508.09640](https://arxiv.org/abs/2508.09640) (2025).

[157] A. Sinibaldi, A. F. Mello, M. Collura, and G. Carleo, Non-stabilizerness of neural quantum states, [arXiv:2502.09725](https://arxiv.org/abs/2502.09725) (2025).

[158] M. Collura, J. D. Nardis, V. Alba, and G. Lami, The non-stabilizerness of fermionic gaussian states, [arXiv:2412.05367](https://arxiv.org/abs/2412.05367) (2025).

[159] B. Dóra and C. P. Moca, Momentum space nonstabilizerness for the transverse field quantum ising model, *Phys. Rev. B* **112**, 125427 (2025).

[160] J. Odavić, T. Haug, G. Torre, A. Hamma, F. Franchini, and S. M. Giampaolo, Complexity of frustration: A new source of non-local non-stabilizerness, *SciPost Phys.* **15**, 131 (2023).

[161] M. A. Rajabpour, Stabilizer-shannon renyi equivalence: Exact results for quantum critical chains, [arXiv:2509.10700](https://arxiv.org/abs/2509.10700) (2025).

[162] R. Ueno, A. Ito, Y. Todo, A. Inoue, K. Minematsu, H. Ishikawa, and N. Homma, All you need is xor-convolution: A generalized higher-order side-channel attack with application to xex/xe-based encryptions, *IACR Transactions on Cryptographic Hardware and Embedded Systems* **2025**, 317–360 (2025).

[163] T. N. Georges, B. K. Berntson, C. Sünderhauf, and A. V. Ivanov, Pauli decomposition via the fast walsh-hadamard transform, *New Journal of Physics* **27**, 033004 (2025).

[164] X. Turkeshi, A. Dymarsky, and P. Sierant, Pauli spectrum and nonstabilizerness of typical quantum many-body states, *Phys. Rev. B* **111**, 054301 (2025).

[165] J. Odavić, M. Viscardi, and A. Hamma, Stabilizer entropy in nonintegrable quantum evolutions, *Phys. Rev. B* **112**, 104301 (2025).

[166] S.-X. Zhang, J. Allcock, Z.-Q. Wan, S. Liu, J. Sun, H. Yu, X.-H. Yang, J. Qiu, Z. Ye, Y.-Q. Chen, C.-K. Lee, Y.-C. Zheng, S.-K. Jian, H. Yao, C.-Y. Hsieh, and S. Zhang, Tensorcircuit: a quantum software framework for the nisq era, *Quantum* **7**, 912 (2023).